

Time-frequency equivalence using chirp signals for frequency response analysis

Resmi Suresh^{a,1} and Raghunathan Rengaswamy^{b,1}

^aIndian Institute of Technology Guwahati, India; ^bIndian Institute of Technology Madras, India

This manuscript was compiled on April 11, 2022

Frequency response analysis (FRA) of systems is a well-researched area. For years, FRA has been performed using input signals, which are a series of sinusoids or a sum of sinusoids. This results in large experimentation time, particularly when the system has to be probed at lower frequencies. In this work, we describe a previously unknown time-frequency duality for linear systems when probed through chirp signals. We show that the entire frequency response can be extracted with a single chirp signal by extending the notion of instantaneous frequency to both the input and output signals. It is surprising that this powerful result had not been uncovered given that FRA has been used in multiple disciplines for more than hundred years. This result has the possibility of completely revolutionizing methods used for frequency response analysis. Theoretical and simulation studies that support the main result are described. While this result is of relevance in multiple areas, we demonstrate the potential impact of this result in electrochemical impedance spectroscopy.

Frequency Response Analysis | Impedance | Chirp signals | EIS |

A system can be characterized by how it responds to sinusoidal input perturbations, also known as the frequency response analysis (FRA). The frequency response at a particular frequency can be specified as a ratio of the output to input, represented as a complex number. Since frequency response is computed from time series data, an equivalence between time and frequency needs to be established. This is directly realized through the well-known Fourier Transform, which allows any time domain signal to be decomposed into its constituent frequency components. A standard approach for FRA of a system is to perturb the system with an input, which is usually a series of sine signals or a sum of sine (multi-sine) signal (1, 2) and identify the frequency response from the output data. A key observation here is that to generate one point in the frequency domain, all the time domain data needs to be processed. This is referred to as the localization problem. A direct consequence of this problem is that large experimentation times are needed for generating the complete frequency response of the system and there are also other issues related to deconvolution of the various frequency components from the time domain signal.

There have been several attempts that have been made over the years to address the localization problem (3, 4). The ideal case would be for a single time point to be localized to a single frequency, which is theoretically not possible. Short term Fourier transforms (STFT) (5) and Wavelet transforms (WT) (3, 4) are some of the time frequency localization approaches that have been attempted. Hilbert-Huang-Transforms (HHT) is another approach that is focused on addressing this problem (6). In HHT, from a time domain signal, the so called intrinsic mode functions (IMF) are extracted, which are as close to monochromatic as possible. Hilbert transforms of the IMF then provide some measure of time frequency lo-

calization. However, none of these techniques (STFT, WT, HHT) specifically focus on generating an exact time frequency equivalence.

Another approach towards time frequency localization is the use of chirp signals (7–10). The interest in chirp signals is due to the fact that it is possible to define a "so called" instantaneous frequency, which is a differential of the phase function of a sinusoid. As a result, a notional frequency can be assigned to every time point in the input signal. Although this notion of one-to-one mapping between time and frequency could be carried over to the output response for linear systems, work in extant literature is focused exclusively on using chirp signals for data generation to be processed by other techniques such as STFT (11–13) or WT (14) and less on exploring the implications of the interesting time-frequency localization that chirp signals afford. This might also be because instantaneous frequency as a concept itself is not well accepted and/or understood (15, 16). There has been interest in interpreting instantaneous frequency and exploring connections between standard techniques such as FFT and chirp, but still only in terms of information content in the signal and not from viewing two time series (input and output) as having the same frequency variation across time (16, 17). Our prior work (18, 19) comes closest to exploring the time-frequency equivalence proposed here; however, we just proposed an algorithm for FRA of electrochemical systems. We claimed that our algorithm was an approximate method for FRA; the impact of time-frequency equivalence was neither clearly understood nor carefully explored at that time. Summarizing, a fundamental question that is of interest is the following: is there a direct one-to-one equivalence between the time domain behavior and the frequency domain behavior that can be established by assigning a single frequency to every time point in a time series data? In this paper, we describe an unexplored equivalence in the case of linear systems when the two time series

Significance Statement

Hundreds of applications utilize frequency response characterization of a system. Identification of frequency response requires long experimentation time, use of transformation techniques and other difficulties associated with isolating the system behavior precisely at individual frequencies. In this work, we report a hitherto unknown result that can be leveraged to mitigate these difficulties resulting in a tremendous reduction in the experimentation time. This result has the possibility of revolutionizing how frequency response studies are performed.

¹To whom correspondence should be addressed. E-mail: raghur@iitm.ac.in, resmis@iitg.ac.in

data (input and output) are hypothesized to possess the same one-to-one time-frequency mapping. This equivalence allows the direct computation of the frequency characteristics from time domain data without ever performing any transformations. It also substantiates the usefulness of the previously hypothesized instantaneous frequency. Finally, the result is an asymptotic result, much in the same format as the well-known time frequency equivalence result for a single frequency input perturbation.

1. Preliminaries

A chirp signal is a signal with time-varying frequency. The generic form of a chirp signal is $u(t) = A \sin(\phi(t))$ where $\phi(t)$ is the instantaneous phase. The instantaneous angular frequency of the signal at any instant t is defined as the differential of the instantaneous phase of the sinusoid at time t ($\omega(t) = 2\pi f(t) = d\phi(t)/dt$). One can see from the definition of chirp signal that the phase function $\phi(t)$ is not assumed to take any particular form. Linear chirp defined below has been a popular choice.

$$\text{Linear Chirp: } u(t) = \sin(\phi_0 + 2\pi(f_0 t + 0.5h_1 t^2)) \quad [1]$$

where $f(t) = f_0 + h_1 t$ is the linear instantaneous frequency and ϕ_0 is the initial phase. One could generalize this linear chirp to n^{th} order polynomial chirp, whose phase function $\phi(t) = P_{n+1}(t)$, is an $(n+1)^{th}$ order polynomial.

2. Results and Discussions

We start with a very well-known result in the area of system identification.

Lemma 1. *When a stable, strictly causal linear system $G(s)$ is perturbed with an input sine signal ($u_s(t) = A_{in} \sin \omega t$; $\omega = 2\pi f$), as time t tends to infinity, output of the system $x(t)$ is also a sine signal with the same frequency as the input but with an amplitude ratio and phase lag.*

$$x(t) = A_{in} AR(\omega) \sin(\omega t + \phi_L(\omega)) + E(t) \quad [2]$$

where $AR(\omega)$ and $\phi_L(\omega)$ are the amplitude ratio and phase lag at angular frequency ω . Also, $E(t) = 0$ and thus,

$$x(t) = A_{in} AR(\omega) \sin(\omega t + \phi_L(\omega)) \quad [3]$$

Remark 1. *This result has been used for decades now and is the foundation on which FRA has progressed. Using this result, the frequency response of the system as a complex number can be identified at each frequency by perturbing the system at every frequency of interest. However, a major disadvantage of this result is that, to derive the complete frequency response, the system has to be perturbed at several frequencies individually. This is sometimes simplified using a sum of sines input and deconvolution of the output using fast Fourier transform (FFT) (20). Notice that this is an asymptotic result and hence one would have to wait for a certain amount of time for the transients to dissipate before the frequency response is identified. We now present the main result derived in this paper and contrast that with Lemma 1.*

Main Result. *When a stable, strictly causal linear system $G(s)$ is perturbed with a chirp signal ($u(t) = A_{in} \sin \phi(t)$), as time t tends to infinity, the output of the system is also a chirp signal such that the instantaneous amplitude ratio (AR^{ch}) and phase lag (ϕ_L^{ch}) of the chirp signal are same as the true amplitude ratio and phase lag of the system corresponding to the instantaneous frequency.*

$$x(t) = A_{in} AR^{ch}(t) \sin(\phi(t) + \phi_L^{ch}(t)) + E^{ch}(t) \quad [4]$$

$$AR^{ch}(t) \Big|_{t=\psi^{-1}(\omega)} = AR(\omega) \quad [5]$$

$$\phi_L^{ch}(t) \Big|_{t=\psi^{-1}(\omega)} = \phi_L(\omega) \quad [6]$$

$$E^{ch}(t) = 0 \quad [7]$$

Angular frequency, $\omega = \psi(t) = \frac{d\phi(t)}{dt}$, is a known quantity from the one-to-one mapping between time and frequency of the input chirp signal.

In summary, the asymptotic output response of the system to an input chirp signal can be written as:

$$x(t) = A_{in} AR(\psi(t)) \sin(\phi(t) + \phi_L(\psi(t))) \quad [8]$$

Remark 2. *The first thing to notice about the main result is that this is also an asymptotic result (much like Lemma 1), where a certain time profile for the output remains after the transients vanish. However, the final time profile that is shown to be retained is the key difference between Lemma 1 and the main result. In Lemma 1, the time profile is a sinusoid of a fixed frequency and a constant amplitude and phase lag. However, in the main result, the time profile is a chirp signal with time varying frequency, amplitude and phase. Let us remember that the differential of the phase of the sinusoid (time function) was defined as the instantaneous frequency at a time point. The amplitude and phase of the output are time functions. Since we have an one-to-one equivalence between time and frequency, we can replace the time variable in the expressions for magnitude and phase with the corresponding frequency function. This would result in magnitude and phase becoming functions of frequency.*

Remark 3. *The main result now provides a remarkable equivalence in that the frequency functions so derived from the output time profiles are exactly equal to the corresponding frequency response functions that would have resulted from applying Lemma 1 for multiple frequencies, once transients vanish. In other words, we now have one frequency defined for every time point and incredibly, all the frequency information is located at that time point. Of course, it is important to reiterate that this is an asymptotic property (like Lemma 1); however, we will demonstrate that the error vanishes very rapidly, making this result of tremendous practical value much like the result described in Lemma 1, which has been used for decades now.*

Remark 4. *The most important implication of this result is that the time required for identifying the FR of the system can be brought down dramatically. This is illustrated in Figure 1, where one sees that a single point in the Nyquist plot corresponds to a signal in FR analysis. In the series of sines approach, these signals are combined serially and this*

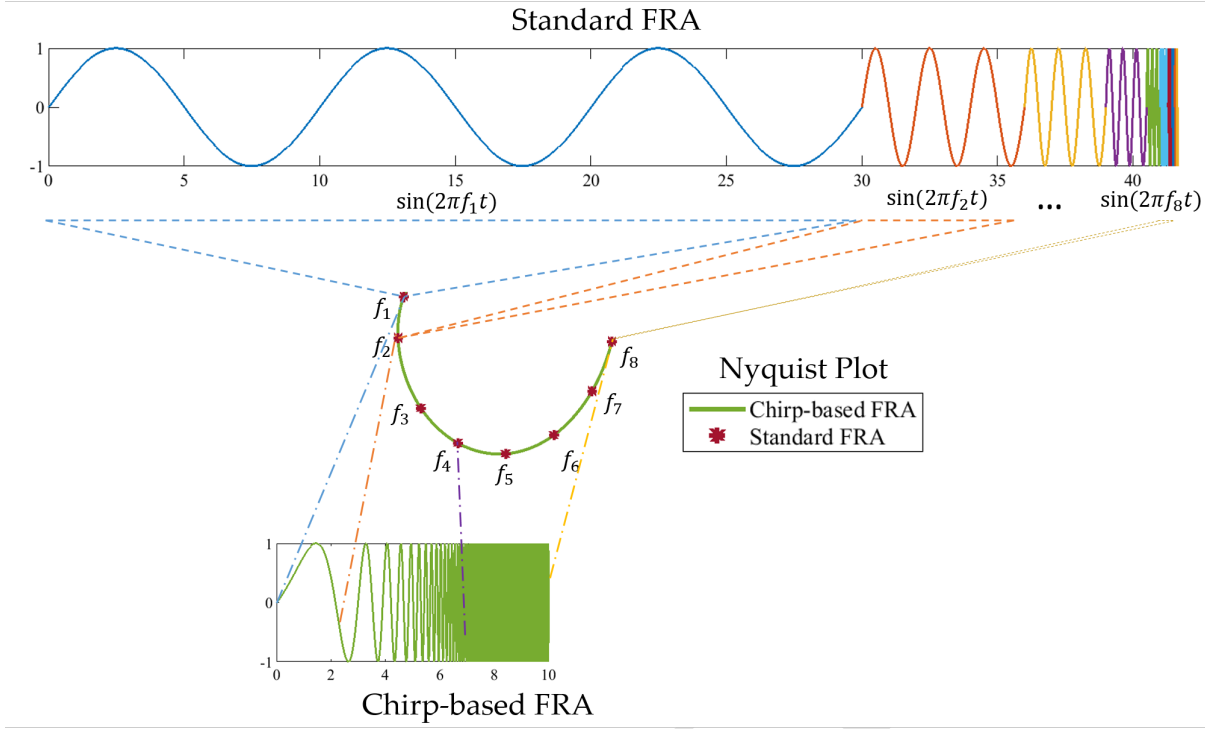


Fig. 1. Comparison of the working of standard FRA and chirp-based FRA. Standard FRA uses a few cycles of multiple sinusoidal signals of different frequencies to obtain discrete points in the Nyquist plot. Chirp-based FRA generates as many points in Nyquist plot as the number of samples in the output signal and thus, a smooth and continuous impedance profile is obtained in a short time.

increases the testing times significantly. In the sum of the sines approach, these signals are overlaid; however, to generate a point in the Nyquist plot, the output has to be deconvolved as responses to each of these sine signals and issues related to spectral leakage and other difficulties need to be addressed (1, 20). Further, the length of the signal is determined by the lowest frequency that one is interested in exploring. The main result in this paper provides us a totally new approach to solving this problem, wherein a single time point in the input signal corresponds to one point in the Nyquist plot (Figure 1). This allows the exploration of multiple frequencies in dramatically reduced experimentation time.

Remark 5. We have presented the key statement of the main result here. All the theoretical underpinnings and a proof for this result for general linear systems with repeated and non-repeated poles along with conditions on admissible phase functions are all comprehensively described in the appendix of this paper. One can see that many functional forms can satisfy the conditions for admissible phase function; however, from a practical demonstration viewpoint we will focus on polynomial chirp signals in this paper.

Based on the *main result*, it is now possible to extract the entire frequency response using a single chirp perturbation experiment unlike standard FRA, where 'n' sinusoidal perturbation experiments would be required to acquire frequency information for 'n' different frequencies with a series of sines. As discussed already, if a multi-sine signal were to be used, the time required would still be dictated by the smallest frequency of interest. As a corollary to the *main result*, a procedure for generating the Nyquist plot (polar representation of the

frequency response obtained by expressing amplitude ratio and phase lag as a complex number) can be developed as shown below:

1. Perturb the system with a chirp input signal of amplitude A_{in} and collect the system's response
2. Obtain the outer envelope of output signal to obtain A^{ch}
3. Calculate amplitude ratio, $AR^{ch} = \frac{A^{ch}}{A_{in}}$
4. Calculate output phase ($\phi + \phi_L^{ch}$) using Eq. (8)
5. Unwrap the output phase to a smooth monotonically increasing function
6. Calculate phase lag, ϕ_L^{ch} , by subtracting the input phase (ϕ) from the output phase obtained in Step 4
7. Generate Nyquist plot using the complex number, $z(\omega) = AR^{ch}(\omega)e^{i\phi_L^{ch}(\omega)}$

We will now validate the claims proposed in this paper through simulation studies. While we have validated the claims on a large number of linear systems with different characteristics, we report results for six different systems of various characteristics in terms of zeros, poles (repeated and not repeated), and orders as shown in Table 1. To validate the claim, we compare the true chirp response ($x(t)$) of these systems to unit amplitude chirp input and the asymptotic output behavior $x(t)$ as predicted by Eq. (8) in Figure 2. Responses corresponding to both linear and fourth order chirp inputs are provided. Linear chirp input

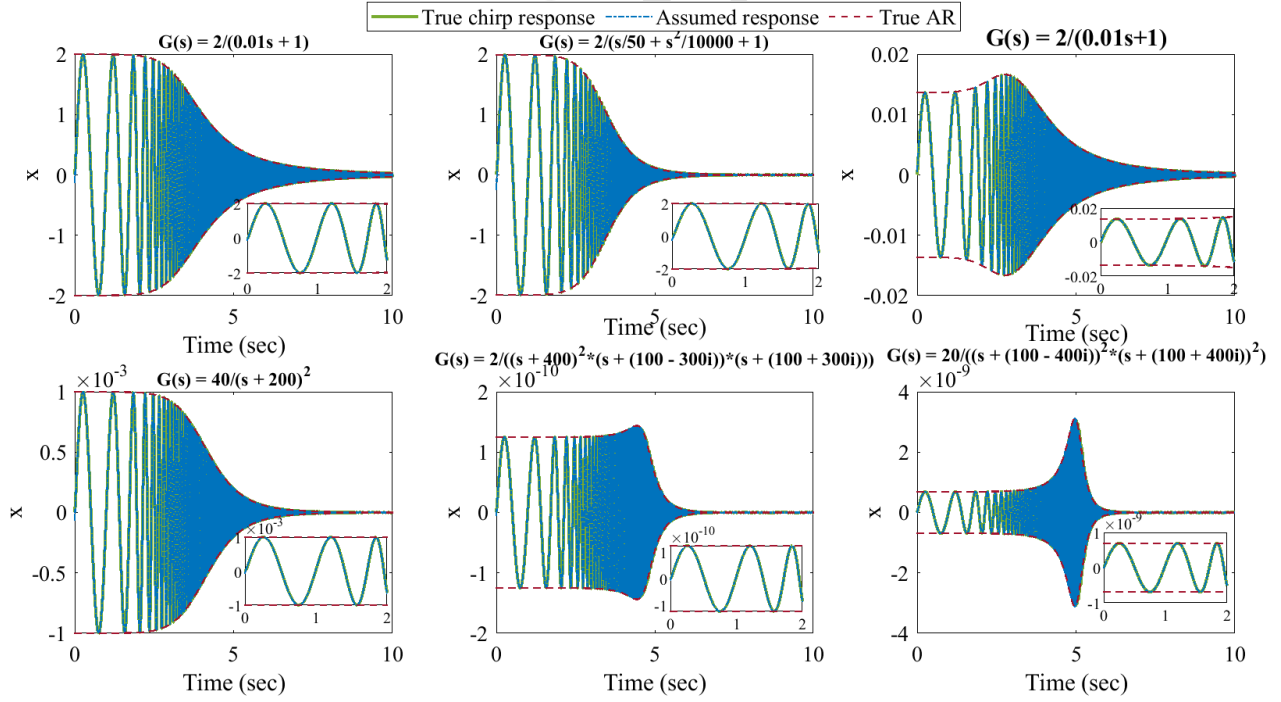
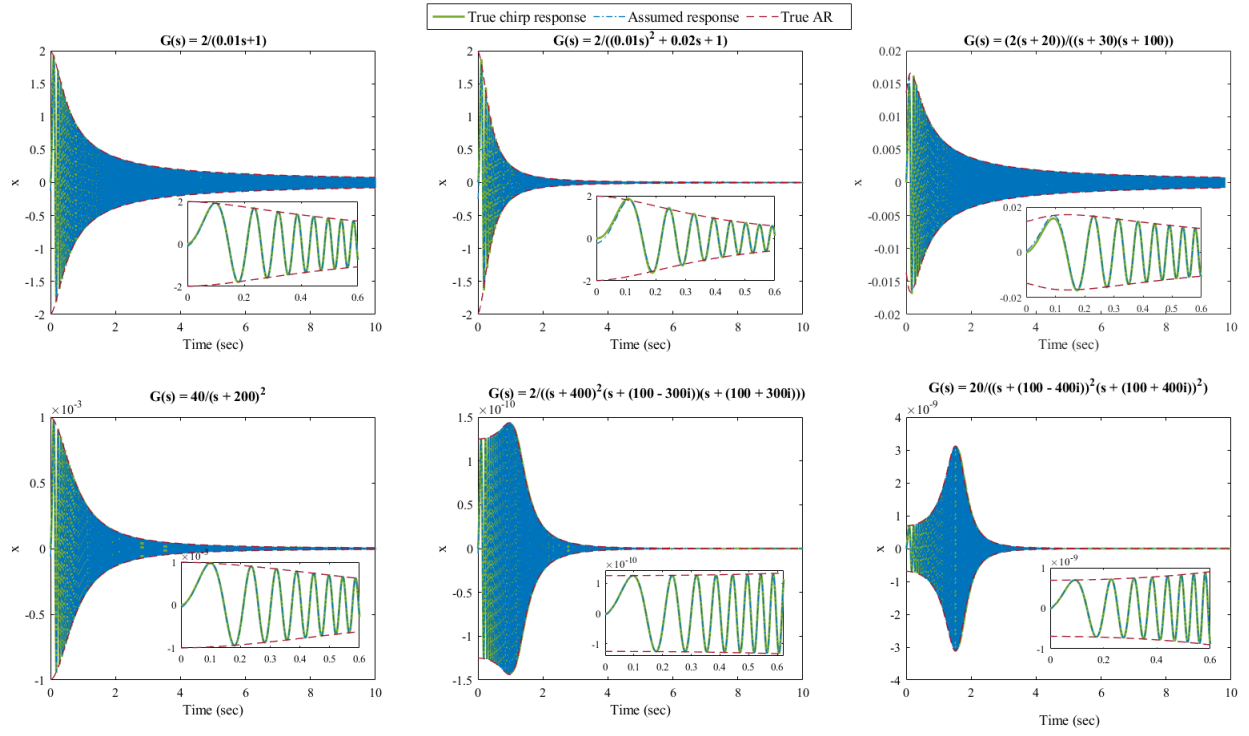


Fig. 2. Response of various systems to linear and fourth order chirp inputs. Zoomed responses are given in the inset.

Table 1. Example systems

Sl.no	System	Remarks
1	$\frac{2}{0.01s+1}$	First-order system
2	$\frac{2}{(0.01s)^2+0.02s+1}$	Second-order critically damped system
3	$\frac{2(s+20)}{(s+100)(s+30)}$	Second-order overdamped system with a zero in left half plane
4	$\frac{40}{(s+200)^2}$	System with real repeated poles
5	$\frac{2}{(s+400)^2(s^2+200s+10000)}$	4 th -order system with real repeated poles and complex conjugate poles
6	$\frac{20}{(s+100+400i)^2(s+100-400i)^2}$	4 th -order system with repeated complex-conjugate pairs as poles

Table 2. Number of articles found since 2018 with the keyword ‘Electrochemical Impedance Spectroscopy’

Google Scholar	ScienceDirect	Scopus
44,603	38,727	59,856

signal that is used sweeps frequencies from 1 Hz to 400 Hz in 10 seconds, while the fourth order chirp input used for the study sweeps frequencies from 1 Hz to 1000 Hz in 10 seconds. An immediate observation from Figure 2 is that in both cases, the envelope of $x(t)$ converges to the true AR and $x(t)$ converges to $x(t)$, very rapidly, within a couple of cycles. To illustrate this, the error $(x(t) - x(t))$ is plotted in Figure 3 for both linear and fourth order chirp responses. It can be seen that the error converges to zero within a short time for both linear and fourth order chirp signals.

The choice of the phase function does have an effect on the speed at which the errors might vanish. However, remarkably, the one-to-one time frequency relationship is retained for different phase functions. The theoretical analysis and the proofs presented in the Appendix describe the mathematics that underlie these observations. The Nyquist plots generated for these examples are provided in Figure 4. It can be seen that the Nyquist profiles match the theoretically computed ones extremely accurately. The chirp signal-based FRA using more than 50000 samples takes approximately 0.25 seconds in an eighth generation i7 processor and thus, is not computationally expensive. It can also be seen that response for a larger frequency range is obtained using a fourth order chirp compared to a linear chirp signal in the same duration. However, for the same experimentation time, within the range of frequency covered by the linear chirp, the resolution will be better for the linear chirp than the fourth order chirp. These simulation results demonstrate the significant application potential for chirp-based FRA.

3. Relevance to Electrochemical Impedance Spectroscopy

While FRA is used in almost all engineering fields, in this section, we will show the relevance of the theoretical developments reported in this paper for electrochemical impedance spectroscopy (EIS). The notion of impedance has been around since the late 1800s with impedance being defined for the first time by Oliver Heaviside and this quantity represented as a complex number by Arthur Kennelly in the 1890s (21). EIS is essentially FRA of systems with the input and output being current and voltage respectively. EIS has been used for diagnostics in various electrochemical systems finding applica-

Table 3. Comparison of standard EIS and chirp signal-based EIS with fourth order chirp input that sweeps through the frequency range [0.001Hz 10000Hz] at a sampling rate, $r = 10,000$ samples/sec.

	Standard EIS	Chirp signal-based EIS
Input signal	$A_{in} \sin(2\pi ft)$	$A_{in} \sin(\phi(t)); \phi = P_5(t); f = \frac{d\phi}{dt}$
Output signal (steady-state)	$A_{in} AR \sin(2\pi ft + \phi_L)$	$A_{in} AR^{ch}(t) \sin(\phi(t) + \phi_L^h(t))$
No. of signals needed	60 (Assume)	1
No. of cycles per signal needed	2 (Assume)	-
Signal duration, T	2.66 hours	100 sec
No. of data points in the plot	60	$10^6 (= r \times T)$

Table 4. Comparison of standard EIS and chirp signal-based EIS

	Standard EIS	Chirp signal-based EIS
Input signal	Sinusoidal	Chirp (Linear/Polynomial)
Frequency of input signal	Constant	Varying
No. of signals needed	Depends on the no. of frequencies needed	1
Time required	Depends on the no. of frequencies needed	Depends on the frequency range
No. of data points in the plot	Same as no. of signals	Same as total samples in the signal

tions in disparate problem domains such as corrosion studies (22, 23), sensors (24), biological systems (25, 26), concrete characterization (27, 28), body fat estimation (29), and many others. Impedance as a diagnostic measure cross-cuts almost all engineering and science disciplines. In view of this universality and continued relevance, there have been thousands of papers that have been devoted to this field. The number of articles with the keyword ‘Electrochemical Impedance Spectroscopy’ is given in Table 2, which is just for a two year period from 2018.

We are now in a position to describe the impact of the *main result* reported in this paper on EIS. If the chirp analysis procedure is followed instead of a series of sinusoidal signals for EIS, then the significance will become apparent. Table 3 outlines the advantages of chirp signals for EIS assuming a frequency range 1 mHz to 10 kHz with a sampling rate of 10000 samples/sec and a fourth order chirp signal. It can be seen that chirp analysis will require only 100 seconds to extract impedance information for 10^6 different frequencies, while standard EIS analysis would require 2.66 hours to extract the impedance information for 60 different frequencies. Table 4 summarizes the main features of the chirp signal-based EIS.

4. Conclusions

In summary, a novel result of this work is that it is possible to extract the entire frequency response from short-term time signals. This result is supported through theoretical analysis and extensive simulation results. The analysis provides an initial assessment of the rate of convergence of the error term. We have verified this result for a large number of linear systems with different characteristics (in terms of zeros and poles) and provide a theoretical proof of its validity for any general linear system (in the Appendix). The relationship between error convergence rates and the choice of phase functions should be more carefully explored. Further, the implications of this approach *vis a vis* the notion of harmonics in frequency response analysis of nonlinear systems need to be explored. Additionally, we have considered monotonically increasing frequency functions, similar analysis needs to be performed for non-monotonic functions. This can open up new ideas for simple nonlinearity detection techniques purely from the response to an appropriately designed chirp signal. Further, the implications of this result from a general system identification viewpoint needs to be assessed. While it has been shown, conceptually, that the whole frequency response can be extracted with large bandwidth short-time signals, there are several practical implementation issues that need to be addressed. These are concerns related to the effect of noise, sampling rates, and non-stationarities. Some of our initial work has started to address these practical implementation issues (18, 19). More sophisticated iterative algorithms for processing the chirp response data can be developed that can minimize, even more, the effect of error terms in the initial

segment of data and the corresponding frequency response identification.

Other than the literature associated with system identification, the approach described in this paper has a role to play in all fields where impedance is used. Impedance being a fundamental characteristic of the system, has been used in various applications (23, 26, 28); however, many of these studies were limited to higher frequencies ($> 1\text{Hz}$) as the time required for impedance generation at low frequencies is usually unacceptably large. Since the impedance information from chirp analysis is obtained in a much shorter time (even at low frequencies), chirp analysis has the potential to become the technique of choice for EIS in all of these applications.

A. Appendix

In this section, we provide theoretical proofs that support the main result. In these proofs, mainly to simplify algebra, we abuse notation a little bit and treat the poles of the transfer function as real numbers. However, all the manipulations are valid for complex poles also. While showing that error terms tend to zero, when we assume that a pole is negative (stability condition), a corresponding interpretation is that the real part of the pole is negative and all the arguments can be shown to be valid with minor modifications for complex poles also.

Theorem 1. *When a stable, strictly causal linear system $G(s)$ without any repeated poles is perturbed with a chirp signal ($u(t) = A_{in} \sin \phi(t)$) with monotonically increasing frequency that satisfies Eq. (59), as time t tends to infinity, the output of the system is also a chirp signal whose instantaneous amplitude*

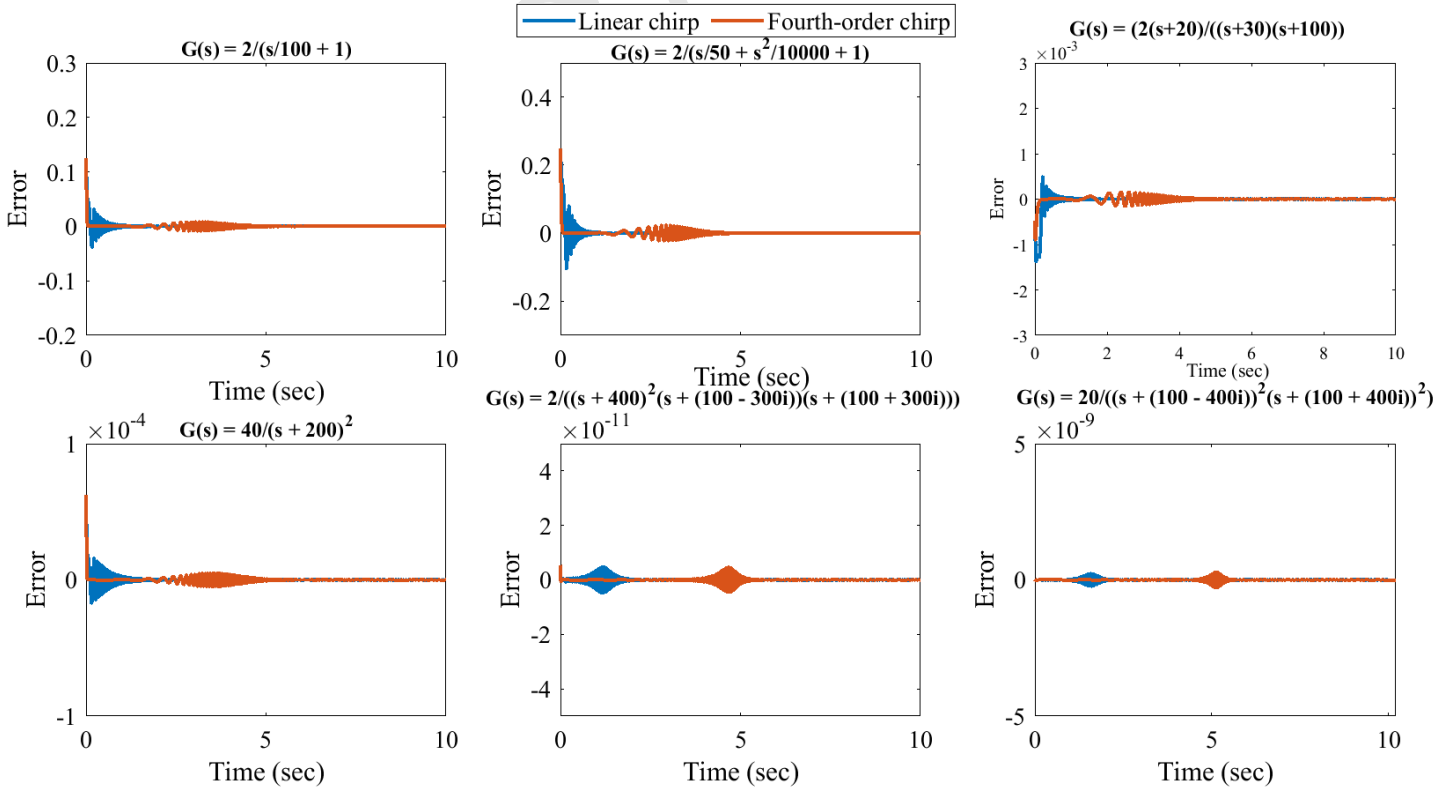
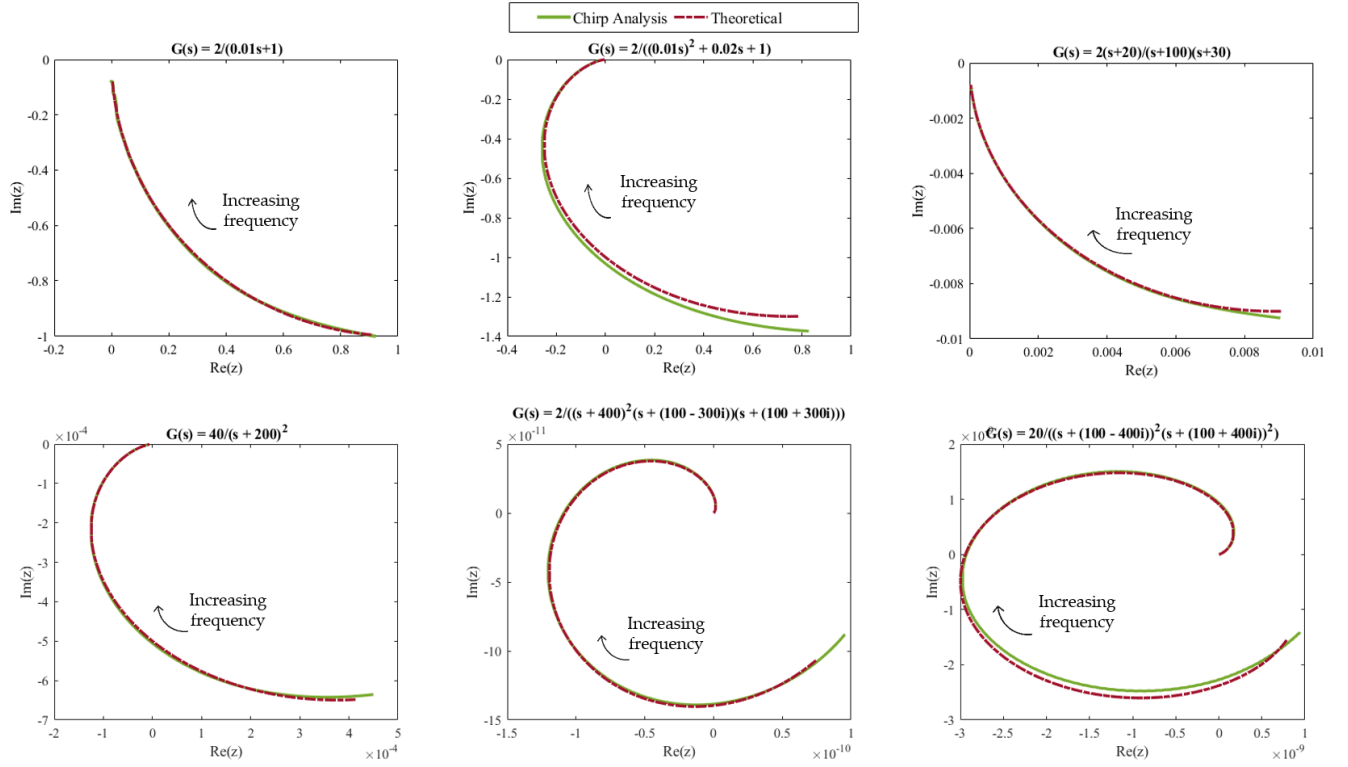
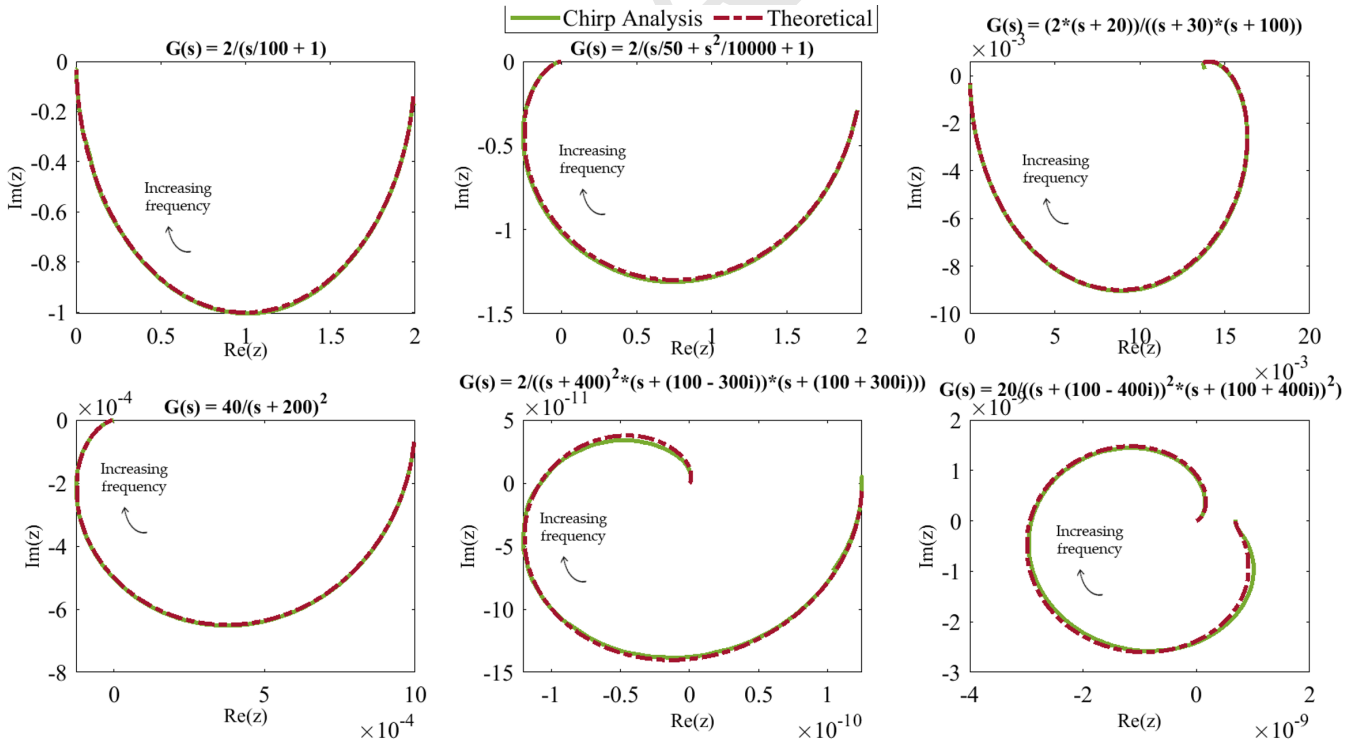


Fig. 3. Error between actual chirp response ($x(t)$) and assumed chirp response $A_{in}AR(\psi(t)) \sin(\phi(t) + \phi_L(\psi(t)))$ for linear and fourth order chirp responses



(a) Nyquist plots generated using linear chirp response



(b) Nyquist plots generated using fourth order chirp response

Fig. 4. Nyquist plots generated using linear and fourth order chirp analysis in comparison with the theoretical frequency response for various systems. Nyquist plots generated using linear and fourth order chirp responses are for the input frequency range [1Hz 400Hz] and [1Hz 1000Hz] respectively.

ratio $\left(AR^{ch} = \frac{A^{ch}}{A_{in}} \text{ where } A^{ch} \text{ is the output chirp amplitude}\right)$ and phase lag (ϕ_L^{ch}) are same as the true amplitude ratio and phase lag of the system corresponding to the instantaneous frequency $(\omega = \frac{d\phi}{dt})$. Mathematically,

$$x(t) = A^{ch}(t) \sin(\phi(t) + \phi_L^{ch}(t)) + E(t) \quad [9]$$

such that

$$AR^{ch}(t)|_{t=\psi^{-1}(\omega)} = AR(\omega) \quad [10]$$

$$\phi_L^{ch}(t)|_{t=\psi^{-1}(\omega)} = \phi_L(\omega) \quad [11]$$

$$E(t)|_{t \rightarrow \infty} = 0 \quad [12]$$

Proof:

The transfer function of a general n^{th} order linear system without repeated roots can be written using partial fraction as follows:

$$G(s) = \frac{X(s)}{U(s)} = \frac{k(s-z_1)(s-z_2)\dots(s-z_m)}{(s-p_1)(s-p_2)\dots(s-p_n)} \quad [13]$$

$$G(s) = \frac{k_1}{(s-p_1)} + \frac{k_2}{(s-p_2)} + \dots + \frac{k_n}{(s-p_n)} \quad [14]$$

$$G(s) = \sum_{q=1}^n \frac{k_q}{(s-p_q)} = \sum_{q=1}^n k_q G_q(s) \quad [15]$$

where $G_q = \frac{1}{(s-p_q)} \quad \forall \quad q \in [1, n]$. The response of this system to any input $u(t)$ whose Laplace transform is $U(s)$ is given by

$$X(s) = G(s)U(s) = \sum_{q=1}^n k_q G_q(s)U(s) \quad [16]$$

$$x(t) = \mathcal{L}^{-1}(G(s)U(s)) = \sum_{q=1}^n k_q \mathcal{L}^{-1}(G_q(s)U(s)) \quad [17]$$

For frequency response analysis, we perturb the system with a sinusoidal input $u_s(t) = A_{in} \sin(\omega t)$. Applying Lemma 1 on the above equation, the asymptotic response of the system to the input $u_s(t)$ can be written as

$$x(t) = A_{in} AR(\omega) \sin(\omega t + \phi_L(\omega)) + E(t) = \sum_{q=1}^n \left(k_q A_{in} AR_q(\omega) \sin[\omega t + \phi_{L,q}(\omega)] + k_q E_q(t) \right) \quad [18]$$

where AR_q and $\phi_{L,q}$ are the true amplitude ratio and phase lag of the system $G_q(s)$, $E(t) = \sum_{q=1}^n k_q E_q(t)$, $E_q = 0$ for all $q \in [1, n]$, and $E|_{t \rightarrow \infty} = 0$.

Now, let us consider the same system being excited using an input chirp signal $u_c(t) = A_{in} \sin(\phi(t))$ with the time-frequency mapping $\omega = \psi(t)$ and Laplace transform $U_c(s)$. Using Lemma 2, we have

$$\mathcal{L}^{-1}(G_q(s)U_c(s)) = A_{in} AR_q(\psi(t)) \sin[\phi(t) + \phi_{L,q}(\psi(t))] + E_q^{ch} \quad \forall q \in [1, n] \quad [19]$$

where $E_q^{ch}(t) = 0$, and $AR_q(\psi(t))$ and $\phi_{L,q}(\psi(t))$ are the true amplitude ratio and phase lag of the system G_q at $\omega =$

$\psi(t)$, which are calculated from the magnitude and phase of $G_q(i\psi(t))$. Substituting in Eq. (17),

$$x(t) = \sum_{q=1}^n \left(k_q A_{in} AR_q(\psi(t)) \sin[\phi(t) + \phi_{L,q}(\psi(t))] \right) + E^{ch}(t) \quad [20]$$

where $E^{ch}(t) = \sum_{q=1}^n k_q E_q^{ch}$. Since $E_q^{ch}(t) = 0$ for all q , $E^{ch}(t) = 0$. At a specific time t_0 ($t_0 \gg 0$), let the ω be $\omega_0 (= \psi(t_0))$ and ϕ is ϕ_0 . Eq. (20) at t_0 ,

$$x(t)|_{t=t_0} = \sum_{q=1}^n k_q A_{in} AR_q(\omega_0) \sin[\phi + \phi_{L,q}(\omega_0)] \quad [21]$$

Comparing with Eq. (18) for $\omega = \omega_0$, the same algebraic manipulations that result in the equivalence in Eq. (18) will lead to the following result:

$$x(t)|_{t=t_0} = A_{in} AR(\omega_0) \sin[\phi + \phi_L(\omega_0)] \quad [22]$$

Since this is true for any $t_0 \gg 0$, it can be concluded that

$$x(t) = A_{in} AR(\psi(t)) \sin[\phi(t) + \phi_L(\psi(t))] + E^{ch}(t) \quad [23]$$

where $E^{ch}(t) = 0$. This completes the proof.

Theorem 2. When a stable, strictly causal linear system $G(s)$ with repeated roots is perturbed with a unit amplitude chirp signal ($u(t) = A_{in} \sin \phi(t)$) with monotonically increasing frequency such that ϕ satisfies the conditions in Eq. (59) and Eq. (83), as time t tends to infinity, the output of the system is also a chirp signal such that the instantaneous amplitude ratio $\left(AR^{ch} = \frac{A^{ch}}{A_{in}} \text{ where } A^{ch} \text{ is the output chirp amplitude}\right)$ and phase lag (ϕ_L^{ch}) of the chirp signal converges to the true amplitude ratio and phase lag of the system corresponding to the instantaneous frequency as t tends to infinity. Mathematically,

$$x(t) = A^{ch}(t) \sin(\phi(t) + \phi_L^{ch}(t)) + E(t) \quad [24]$$

such that

$$\lim_{t \rightarrow \infty} AR^{ch}(t)|_{t=\psi^{-1}(\omega)} = AR(\omega) \quad [25]$$

$$\lim_{t \rightarrow \infty} \phi_L^{ch}(t)|_{t=\psi^{-1}(\omega)} = \phi_L(\omega) \quad [26]$$

$$E(t)|_{t \rightarrow \infty} = 0 \quad [27]$$

Proof:

A general n^{th} order linear system with transfer function $G(s) = \frac{X(s)}{U(s)}$ can be written using partial fraction as follows:

$$G(s) = \frac{X(s)}{U(s)} = \frac{k(s-z_1)(s-z_2)\dots(s-z_m)}{(s-p_1)^{n_1}(s-p_2)^{n_2}\dots(s-p_r)^{n_r}} \quad [28]$$

$$G(s) = \frac{k_{1,1}}{(s-p_1)} + \frac{k_{1,2}}{(s-p_1)^2} + \dots + \frac{k_{1,n_1}}{(s-p_1)^{n_1}} + \frac{k_{2,1}}{(s-p_2)} + \dots + \frac{k_{r,n_r}}{(s-p_r)^{n_r}} \quad [29]$$

such that $n = n_1 + n_2 + \dots + n_r$. We can simplify the equation for $G(s)$ as follows:

$$G(s) = \sum_{q=1}^r \sum_{m=1}^{n_q} \frac{k_q}{(s-p_q)^m} = \sum_{q=1}^r \sum_{m=1}^{n_q} k_q G_{q,m}(s) \quad [30]$$

where $G_{q,m}(s) = \frac{1}{(s-p_q)^m}$. The response of this system to any input $u(t)$ whose Laplace transform is $U(s)$ is given by

$$X(s) = G(s)U(s) = \sum_{q=1}^r \sum_{m=1}^{n_q} k_q G_{q,m}(s)U(s) \quad [31]$$

$$x(t) = \mathcal{L}^{-1}(G(s)U(s)) = \sum_{q=1}^r \sum_{m=1}^{n_q} k_q \mathcal{L}^{-1}(G_{q,m}(s)U(s)) \quad [32]$$

For frequency response analysis, we perturb the system with a sinusoidal input $u_s(t) = A_{in} \sin(\omega t)$. Applying Lemma 1 on the above equation, the asymptotic response of the system to the input $u_s(t)$ can be written as

$$\begin{aligned} x(t) &= \sum_{q=1}^r \sum_{m=1}^{n_q} (k_q A_{in} AR_{q,m}(\omega) \sin[\omega t + \phi_{L,q,m}(\omega)] \\ &\quad + k_q E_{q,m}(t)) \\ &= A_{in} AR(\omega) \sin(\omega t + \phi_L(\omega)) + E(t) \end{aligned} \quad [33]$$

such that $E(t) = \sum_{q=1}^r \sum_{m=1}^{n_q} k_q E_{q,m}(t)$, $E(t) = 0$, and $E_{q,m}(t) = 0$. $AR_{q,m}$ and $\phi_{L,q,m}$ are the true amplitude ratio and phase lag of the system $G_{q,m}(s)$.

Let us consider the same system being excited using an input chirp signal $u_c(t) = A_{in} \sin \phi(t)$ with the time-frequency mapping $\omega = \psi(t)$ and Laplace transform $U_c(s)$. Applying Lemmas 2 and 3 in Eq. (32), we have

$$x(t) = \sum_{q=1}^r \sum_{m=1}^{n_q} (k_q A_{in} AR_q \sin[\phi + \phi_{L,q}] + E^{ch}) \quad [34]$$

where $\sum_{q=1}^r \sum_{m=1}^{n_q} k_q E_{q,m}^{ch} = E^{ch}$ and $E_{q,m}^{ch}$ is the error term for the system $G_{q,m}$ that vanishes as t tends to infinity. Since $E_{q,m}^{ch} = 0$ for all q , $E^{ch} = 0$. Using the same arguments presented in the proof of Theorem 1, by comparing the equations Eq. (33) and Eq. (34), we can write

$$x(t) = A_{in} AR^{ch}(\psi(t)) \sin[\phi(t) + \phi_L^{ch}(\psi(t))] + E^{ch}(t) \quad [35]$$

such that $AR^{ch} = AR$, $\phi_L^{ch} = \phi_L$ and $E^{ch} = 0$.

Remark 6. The standard frequency response analysis can be thought of as a corollary of this result where $\phi = \omega t$.

Remark 7. The difference between Theorems 1 and 2 is that when the linear system has no repeated poles, through the conversion of time to frequency, the time functions for amplitude and phase lag are shown to be the same as the frequency functions for amplitude and phase lag at all times (Theorem 1), whereas, when the linear system has repeated poles, the time functions are shown to converge asymptotically to the frequency functions (Theorem 2). It is also worthwhile to reiterate that in both cases, there is an additive error term that vanishes rapidly, similar to the standard FRA result.

Lemma 2. When a stable first-order system $G(s) = \frac{1}{s-p}$ is perturbed with a chirp signal ($u(t) = A_{in} \sin \phi(t)$) with monotonically increasing frequency and when ϕ satisfies the conditions in Eq. (59), as time t tends to infinity, the output of the system is also a chirp signal such that the instantaneous amplitude ratio (AR^{ch}) and phase lag (ϕ_L^{ch}) of the chirp signal are same as the true amplitude ratio and phase lag of the system corresponding to the instantaneous frequency.

$$x(t) = A_{in} AR(\psi(t)) \sin[\phi(t) + \phi_L(\psi(t))] + E(t) \quad [36]$$

where $E(t) = 0$ or simply,

$$x(t) = A_{in} AR(\psi(t)) \sin[\phi(t) + \phi_L(\psi(t))] \quad [37]$$

Remark 8. While Theorem 1 is stated for any stable, strictly causal linear system without repeated poles, this Lemma shows how Theorem 1 works for a general first-order system $G(s) = \frac{1}{s-p}$. This Lemma is used in combination with Lemma 1 and the idea of partial fraction expansion to prove Theorem 1.

Proof:

From the frequency response analysis of $G(s)$, we have the following expressions for the amplitude ratio (AR) and phase lag (ϕ_L) at various frequencies (ω).

$$AR(\omega) = \frac{1}{\sqrt{p^2 + \omega^2}} \quad [38]$$

$$\phi_L(\omega) = \tan^{-1} \left(\frac{-\omega}{-p} \right) \quad [39]$$

Let this system be perturbed by an input chirp signal $u(t) = A_{in} \sin \phi(t)$. The output response is given by

$$\frac{dx}{dt} - px = u \quad [40]$$

Multiplying with e^{-pt} and rearranging,

$$\frac{d}{dt}(e^{-pt}x) = A_{in} e^{-pt} \sin \phi(t) \quad [41]$$

Integrating,

$$e^{-pt}x = \int A_{in} e^{-pt} \sin \phi \, dt + C_1 \quad [42]$$

$$= \frac{A_{in}}{2i} \int e^{-pt} (e^{i\phi} - e^{-i\phi}) dt + C_1 \quad [43]$$

$$= \frac{A_{in}}{2i} \left[\int e^{-pt+i\phi} dt - \int e^{-pt-i\phi} dt \right] + C_1 \quad [44]$$

$$x = \frac{A_{in} e^{pt}}{2i} \left[\int \frac{d(e^{-pt+i\phi})}{-p+i\omega} - \int \frac{d(e^{-pt-i\phi})}{-p-i\omega} \right] + C_1 e^{pt} \quad [45]$$

where $\omega(t) = \frac{d\phi}{dt}$. Since

$$\int \frac{d(e^{-pt \pm i\phi})}{-p \pm i\omega} = \frac{e^{-pt \pm i\phi}}{-p \pm i\omega} - \int e^{-pt \pm i\phi} d \left(\frac{1}{-p \pm i\omega} \right) \quad [46]$$

$$= \frac{e^{-pt \pm i\phi}}{-p \pm i\omega} - \int e^{-pt \pm i\phi} \frac{\mp i \gamma dt}{(-p \pm i\omega)^2} \quad [47]$$

where $\gamma = \frac{d^2\phi}{dt^2}$ is the instantaneous angular chirpiness. Substituting in Eq. (45), we have

$$x = \frac{A_{in}}{2i} \left[\frac{e^{i\phi}}{-p+i\omega} - \frac{e^{-i\phi}}{-p-i\omega} \right] + I_1 + I_2 + C_1 e^{pt} \quad [48]$$

$$= \frac{A_{in}}{(p^2 + \omega^2)} \left[\frac{-p}{2i} (e^{i\phi} - e^{-i\phi}) - \frac{\omega}{2} (e^{i\phi} + e^{-i\phi}) \right] + I_1 + I_2 + C_1 e^{pt} \quad [49]$$

$$= \frac{A_{in}}{(p^2 + \omega^2)} [-p \sin \phi - \omega \cos \phi] + I_1 + I_2 + C_1 e^{pt} \quad [50]$$

where

$$I_1 = \frac{A_{in} e^{pt}}{2} \int e^{-pt+i\phi} \frac{\gamma dt}{(-p+i\omega)^2} \quad [51]$$

$$I_2 = \frac{A_{in} e^{pt}}{2} \int e^{-pt-i\phi} \frac{\gamma dt}{(-p-i\omega)^2} \quad [52]$$

Now,

$$\sin \left(\phi + \tan^{-1} \left(\frac{-\omega}{-p} \right) \right) = \frac{1}{\sqrt{p^2 + \omega^2}} (-p \sin \phi - \omega \cos \phi) \quad [53]$$

Substituting in Eq. (50),

$$x(t) = \frac{A_{in}}{\sqrt{p^2 + \omega^2}} \sin \left[\phi + \tan^{-1} \left(\frac{-\omega}{-p} \right) \right] + E(t) \quad [54]$$

where $E(t) = I_1 + I_2 + C_1 e^{pt}$ is the error between the proposed asymptotic response (given by Eq. (8)) and the true chirp response $x(t)$. To find the asymptotic behavior of $x(t)$ as $t \rightarrow \infty$, we are interested in the asymptotic behavior of the absolute values of the integrals I_1 and I_2 . Using $|e^{i\phi}| = 1$, $|fg| = |f||g|$, $|\int f du| \leq \int |f| du$ and the Hölder's integral inequality, we can write,

$$|I_1| = \left| \frac{A_{in} e^{pt}}{2} \int e^{-pt+i\phi} \frac{\gamma}{(-p+i\omega)^2} dt \right| \quad [55]$$

$$\leq \left| \frac{A_{in} e^{pt}}{2} \int e^{-pt+i\phi} \frac{\gamma}{(-p+i\omega)^2} dt \right| \quad [56]$$

$$\leq \left| \frac{A_{in} e^{pt}}{2} \left(\int_0^{\frac{t}{2}} e^{-pt} \frac{\gamma}{(-p+i\omega)^2} dt \right) + \left| \frac{A_{in} e^{pt}}{2} \left(\int_{\frac{t}{2}}^t e^{-pt} \frac{\gamma}{(-p+i\omega)^2} dt \right) \right| \right| \quad [57]$$

$$\begin{aligned} |I_1| &\leq \frac{|A_{in}| e^{pt}}{2} \left(\int_0^{\frac{t}{2}} e^{-2pt} dt \right)^{\frac{1}{2}} \left(\int_0^{\frac{t}{2}} \left| \frac{\gamma}{(-p+i\omega)^2} \right|^2 dt \right)^{\frac{1}{2}} \\ &+ \frac{|A_{in}| e^{pt}}{2} \left(\int_{\frac{t}{2}}^t e^{-2pt} dt \right)^{\frac{1}{2}} \left(\int_{\frac{t}{2}}^t \left| \frac{\gamma}{(-p+i\omega)^2} \right|^2 dt \right)^{\frac{1}{2}} \\ &\leq \frac{|A_{in}| e^{pt}}{2\sqrt{-2p}} (e^{-pt} - 1)^{\frac{1}{2}} \left(\int_0^{\frac{t}{2}} \left| \frac{\gamma}{(-p+i\omega)^2} \right|^2 dt \right)^{\frac{1}{2}} \\ &+ \frac{|A_{in}| e^{pt}}{2\sqrt{-2p}} (e^{-2pt} - e^{-pt})^{\frac{1}{2}} \left(\int_{\frac{t}{2}}^t \left| \frac{\gamma}{(-p+i\omega)^2} \right|^2 dt \right)^{\frac{1}{2}} \end{aligned} \quad [58]$$

For any chirp input with monotonically increasing frequency and a stable $G(s)$, it can be easily shown that $|I_1| = 0$ as $t \rightarrow \infty$ any function ϕ that satisfies (with $\alpha > \frac{1}{2}$) after some finite time $t \geq T_0$,

$$\left| \frac{d^2\phi}{dt^2} / \left(\frac{d\phi}{dt} \right)^2 \right| \leq \mathcal{O}(1/t^\alpha) \quad [59]$$

Similar results holds for $|I_2|$. Also, for a stable system, $C_1 e^{pt} = 0$, and thus, $E(t) = 0$. Substituting these results in Eq. (54), we get

$$x_{t \rightarrow \infty} = \frac{A_{in}}{\sqrt{p^2 + \omega^2}} \sin \left[\phi + \tan^{-1} \left(\frac{-\omega}{-p} \right) \right] \quad [60]$$

Comparing Eq. (60) with Eq. (38) and Eq. (39), and using the time-frequency mapping $\omega = \psi(t)$, we have

$$x_{t \rightarrow \infty} = A_{in} AR(\psi(t)) \sin [\phi(t) + \phi_L(\psi(t))] \quad [61]$$

Remark 9. Eq. (59) is a sufficiency condition and not shown to be a necessary condition. It can be easily seen that Eq. (59) is satisfied by linear and fourth order chirp signals. One could explore many other functional forms including composite forms that satisfy the conditions as candidate phase functions in a chirp signal.

Remark 10. It can be seen that the rate at which error vanishes will also depend on the choice of phase function corroborating the observations made based on the simulation studies reported in this paper.

Lemma 3. When a stable system with a pole repeated n times, $G(s) = \frac{1}{(s-p)^n}$, is perturbed with a chirp signal ($u(t) = A_{in} \sin \phi(t)$) with monotonically increasing frequency such that ϕ satisfies the conditions in Eq. (59) and Eq. (83), as time t tends to infinity, output of the system is also a chirp signal such that the instantaneous amplitude ratio (AR^{ch}) and phase lag (ϕ_L^{ch}) of the chirp signal will converge to the true amplitude ratio and phase lag of the system corresponding to the instantaneous frequency asymptotically.

$$x(t) = A_{in} AR^{ch}(t) \sin [\phi(t) + \phi_L^{ch}(t)] + E(t) \quad [62]$$

where $AR^{ch}(t) = AR(\psi(t))$, $\phi_L^{ch}(t) = \phi_L(\psi(t))$, and $E(t) = 0$. Consequently,

$$x_{t \rightarrow \infty}(t) = A_{in} AR(\psi(t)) \sin [\phi(t) + \phi_L(\psi(t))] \quad [63]$$

Remark 11. While Theorem 2 is stated for any stable, strictly causal linear system with both repeated poles and non-repeated poles, this Lemma shows how Theorem 2 works for a system with one pole repeated n times $G(s) = \frac{1}{(s-p)^n}$. This Lemma is used in combination with Lemma 1 and the idea of partial fraction expansion to prove Theorem 2.

Proof:

From the frequency response analysis of $G(s) = \frac{1}{(s-p)^n}$, we have the following expressions for the amplitude ratio (AR) and phase lag (ϕ_L) at various frequencies (ω).

$$AR(\omega) = \left(\frac{1}{\sqrt{p^2 + \omega^2}} \right)^n \quad [64]$$

$$\phi_L(\omega) = n \tan^{-1} \left(\frac{-\omega}{-p} \right) \quad [65]$$

Let this system be perturbed by an input chirp signal $u(t) = A_{in} \sin(\phi(t))$. The system can be thought of as a cascade of n steps such that

$$X_q(s) = \frac{1}{(s-p)} X_{q-1}(s) \quad \forall q \in [1, n] \quad [66]$$

Note that $X_0(s)$ is the input Laplace transform $U(s)$. We will now prove *Lemma 3* through induction. Let us assume that *Lemma 3* is true for $G_q(s) = \frac{1}{(s-p)^q}$. Hence, if G_q is perturbed by an input chirp signal of the form $A_{in}(t) \sin(\phi(t))$, the output (x_q) is also a chirp signal of the form $A_q(t) \sin(\phi + \phi_{L,q}(t))$ where

$$A_q = \frac{A_{in}}{(\sqrt{p^2 + \omega^2})^q}; \quad \phi_{L,q} = q \tan^{-1} \left(\frac{-\omega}{-p} \right) \quad [67]$$

Defining $\phi_q = \phi + \phi_{L,q}$, the instantaneous angular frequency and chirpiness of the output are $\omega_q = \frac{d\phi_q}{dt} = \omega + \omega_{L,q}$ and $\gamma_q = \frac{d^2\phi}{dt^2}$ respectively, where

$$\omega_{L,q} = \frac{d\phi_{L,q}}{dt} = \frac{qp \frac{d^2\phi}{dt^2}}{p^2 + (\frac{d\phi}{dt})^2} \quad [68]$$

For any $q+1$, the corresponding differential equation can be written as

$$\frac{dx_{q+1}}{dt} - px_{q+1} = x_q \quad [69]$$

Substituting $x_q = A_q(t) \sin(\phi_q(t))$ and multiplying the equation with e^{-pt} , we have

$$\frac{d}{dt}(e^{-pt} x_{q+1}) = e^{-pt} A_q(t) \sin(\phi_q(t)) \quad [70]$$

Integrating and rearranging,

$$x_{q+1} = e^{pt} \int e^{-pt} A_q(t) \sin(\phi_q(t)) dt + C_2 e^{pt} \quad [71]$$

$$= \frac{e^{pt}}{2i} \int e^{\ln A_q} e^{-pt} (e^{i\phi_q} - e^{-i\phi_q}) dt + C_2 e^{pt} \quad [72]$$

$$= \frac{e^{pt}}{2i} \int \frac{de^{\ln A_q - pt + i\phi_q}}{D_q + i\omega_q} - \frac{de^{\ln A_q - pt - i\phi_q}}{D_q - i\omega_q} + C_2 e^{pt} \quad [73]$$

where

$$D_q = \frac{A'_q}{A_q} - p = \frac{-q\omega\gamma}{p^2 + \omega^2} - p \quad [74]$$

Since,

$$\begin{aligned} & \frac{de^{\ln A_q - pt \pm i\phi_q}}{D_q \pm i\omega_q} \\ &= \frac{e^{\ln A_q - pt \pm i\phi_q}}{D_q \pm i\omega_q} - \int e^{\ln A_q - pt \pm i\phi_q} d \left(\frac{1}{D_q \pm i\omega_q} \right) \\ &= \frac{A_q e^{-pt} e^{\pm i\phi_q}}{D_q \pm i\omega_q} - \int A_q e^{-pt \pm i\phi_q} \frac{-\frac{dD_q}{dt} \mp i\gamma_q}{(D_q \pm i\omega_q)^2} dt \end{aligned} \quad [75]$$

we can rewrite Eq. (73) as follows:

$$x_{q+1} = \frac{A_q}{2i} \left(\frac{e^{i\phi_q}}{D_q + i\omega_q} - \frac{e^{-i\phi_q}}{D_q - i\omega_q} \right) + E(t) \quad [77]$$

where

$$I_3 = \frac{e^{pt}}{2} \int A_q e^{-pt + i\phi_q} \frac{-i \frac{dD_q}{dt} + \gamma_q}{(D_q + i\omega_q)^2} dt \quad [78]$$

$$I_4 = -\frac{e^{pt}}{2} \int A_q e^{-pt - i\phi_q} \frac{-i \frac{dD_q}{dt} - \gamma_q}{(D_q - i\omega_q)^2} dt \quad [79]$$

$$E(t) = I_3 + I_4 + C_2 e^{pt} \quad [80]$$

Following the same steps used in simplifying Eq. (48) to Eq. (54), Eq. (77) can be simplified as follows:

$$x_{q+1} = \frac{A_q}{\sqrt{D_q^2 + \omega_q^2}} \sin \left(\phi + \phi_{L,q} + \tan^{-1} \left(\frac{-\omega_q}{D_q} \right) \right) + E(t) \quad [81]$$

Defining $A_{q+1} = \frac{A_q}{\sqrt{D_q^2 + \omega_q^2}}$ and $\phi_{L,q+1} = \phi_{L,q} + \tan^{-1} \left(\frac{-\omega_q}{D_q} \right)$, we have

$$x_{q+1} = A_{q+1} \sin(\phi + \phi_{L,q+1}) + E(t) \quad [82]$$

To find the asymptotic behavior of $x_{q+1}(t)$ as $t \rightarrow \infty$, we are interested in the asymptotic behavior of A_{q+1} , $\phi_{L,q+1}$, and the absolute values of the integrals I_3 and I_4 . For any input chirp signal with monotonically increasing frequency, which satisfies Eq. (59) and

$$\lim_{t \rightarrow \infty} \left(\frac{\frac{d^2\phi}{dt^2}}{\frac{d\phi}{dt}} \right) = 0 \quad [83]$$

we have the following expressions using equations Eq. (68) and Eq. (74).

$$\omega_{L,q} = \lim_{t \rightarrow \infty} \frac{qp \left(\frac{d^2\phi}{dt^2} \right)}{\left(\frac{d\phi}{dt} \right)^2} = 0 \implies \omega_q = \omega \quad [84]$$

$$D_q = \lim_{t \rightarrow \infty} \frac{-q \left(\frac{d^2\phi}{dt^2} \right)}{\frac{d\phi}{dt}} - p = -p \quad [85]$$

Using the definitions of A_{q+1} and $\phi_{L,q+1}$, for all $q \in [1, n]$, we have,

$$A_{q+1} = \frac{A_q}{\sqrt{p^2 + \omega^2}} = A_{in} \left(\frac{1}{\sqrt{p^2 + \omega^2}} \right)^{q+1} \quad [86]$$

$$\phi_{L,q+1} = \phi_{L,q} + \tan^{-1} \left(\frac{-\omega}{-p} \right) = (q+1) \tan^{-1} \left(\frac{-\omega}{-p} \right) \quad [87]$$

Now, to find the asymptotic behaviors of $|I_3|$, using $|fg| = |f||g|$, $|\int f du| \leq \int |f| du$ and the Hölder's integral inequality on Eq. (78). Also, since $G(s)$ is a strictly proper stable system and A_q is bounded. Let the upper bound of A_q be A_{ub} .

$$\begin{aligned} |I_3| &= \left| \frac{e^{pt}}{2} \int A_q e^{-pt + i\phi_q} \frac{-i \frac{dD_q}{dt} + \gamma_q}{(D_q + i\omega_q)^2} dt \right| \\ &\leq \left| \frac{e^{pt}}{2} \int A_q e^{-pt + i\phi_q} \frac{-i \frac{dD_q}{dt} + \gamma_q}{(D_q + i\omega_q)^2} dt \right| \end{aligned} \quad [88]$$

$$\begin{aligned}
|I_3| &\leq \frac{|A_{ub}e^{pt}|}{2} \int_0^{\frac{t}{2}} \left| e^{-pt} \frac{-i \frac{dD_q}{dt} + \gamma_q}{(D_q + i\omega_q)^2} \right| dt + \\
&\quad \left| \frac{A_{ub}e^{pt}}{2} \right| \int_{\frac{t}{2}}^t \left| e^{-pt} \frac{-i \frac{dD_q}{dt} + \gamma_q}{(D_q + i\omega_q)^2} \right| dt \quad [89] \\
&\leq \frac{|A_{ub}|e^{pt}}{2} \left(\int_0^{\frac{t}{2}} e^{-2pt} dt \right)^{\frac{1}{2}} \left(\int_0^{\frac{t}{2}} \left| \frac{-i \frac{dD_q}{dt} + \gamma_q}{(D_q + i\omega_q)^2} \right|^2 dt \right)^{\frac{1}{2}} \\
&\quad + \frac{|A_{ub}|e^{pt}}{2} \left(\int_{\frac{t}{2}}^t e^{-2pt} dt \right)^{\frac{1}{2}} \left(\int_{\frac{t}{2}}^t \left| \frac{-i \frac{dD_q}{dt} + \gamma_q}{(D_q + i\omega_q)^2} \right|^2 dt \right)^{\frac{1}{2}} \\
&\leq \frac{|A_{ub}|e^{pt}}{2\sqrt{-2p}} (e^{-pt} - 1)^{\frac{1}{2}} \left(\int_0^{\frac{t}{2}} \left| \frac{-i \frac{dD_q}{dt} + \gamma_q}{(D_q + i\omega_q)^2} \right|^2 dt \right)^{\frac{1}{2}} \\
&\quad + \frac{|A_{ub}|e^{pt}}{2\sqrt{-2p}} (e^{-2pt} - e^{-pt})^{\frac{1}{2}} \left(\int_{\frac{t}{2}}^t \left| \frac{-i \frac{dD_q}{dt} + \gamma_q}{(D_q + i\omega_q)^2} \right|^2 dt \right)^{\frac{1}{2}} \quad [90]
\end{aligned}$$

For any chirp input with monotonically increasing frequency with a stable $G(s)$, it can be easily shown that $|I_3| = 0$ for any function ϕ that satisfies Eq. (59) and Eq. (83). Using the same approach, it can be shown that $|I_4| = 0$. Also, for a stable system, $C_2e^{pt} = 0$, and thus, $E(t) = 0$. Substituting these results in Eq. (82), we get

$$x_{q+1} = A_{in} \left(\frac{1}{\sqrt{p^2 + \omega^2}} \right)^{q+1} \sin \left[\phi + (q+1) \tan^{-1} \left(\frac{-\omega}{-p} \right) \right] \quad [91]$$

Lemma 2 establishes that the condition on x_q shown in Eq. (67) is satisfied for $q = 1$. As a result, the induction process ensures that Lemma 3 is valid for any value of n . Hence, the output response of the system $G(s)$ ($x(t) = x_n(t)$) to an input chirp response $A_{in} \sin \phi(t)$ with monotonically increasing frequency such that ϕ satisfies Eq. (59) and Eq. (83) will asymptotically converge to the following form:

$$x(t) = A_{in} \left(\frac{1}{\sqrt{p^2 + \omega^2}} \right)^n \sin \left[\phi + n \tan^{-1} \left(\frac{-\omega}{-p} \right) \right] \quad [92]$$

Comparing Eq. (92) with Eq. (64) and Eq. (65), and using the time-frequency mapping $\omega = \psi(t)$, we have

$$x(t) = A_{in} AR(\psi(t)) \sin [\phi(t) + \phi_L(\psi(t))] \quad [93]$$

Remark 12. Lemma 3 is true for any phase function that satisfies Eq. (59) and Eq. (83). Eq. (59) is already required for Lemma 2. It can be easily seen that Eq. (83) is satisfied for the linear and fourth order chirp signals. Note that while we have separate theorems for linear systems with repeated and non-repeated poles, from an algorithmic viewpoint, there is no difference in how these systems are handled and hence, there is no need to know the type of system being addressed, a priori, while frequency response analysis is performed. Our simulation studies demonstrate this and also the fact that there are no performance differences for the cases of repeated and non-repeated poles.

Remark 13. One another popular chirp signal is the exponential chirp signal given by $u(t) = \sin \left(\phi_0 + 2\pi f_0 \left(\frac{h_2^t - 1}{\ln h_2} \right) \right)$, where $f(t) = f_0 h_2^t$ is the exponentially varying instantaneous frequency. This form has been used in many studies including our work where we show that exponential chirp can be used for EIS (19). While this signal satisfies all conditions for Lemma 2, it does not satisfy Eq. (83), a Lemma 3 condition (needed for repeated roots). However, from a practical application viewpoint, the exponential chirp signal performs very well for systems with non-repeated roots (for which all conditions are satisfied) and repeated roots.

1. E Van der Ouderaa, J Schoukens, J Renneboog, Peak factor minimization using a time-frequency domain swapping algorithm. *IEEE Transactions on Instrumentation Meas.* **37**, 145–147 (1988).
2. B Sanchez, G Vandersteen, R Bragos, J Schoukens, Optimal multisine excitation design for broadband electrical impedance spectroscopy. *Meas. Sci. Technol.* **22**, 115601 (2011).
3. M Itagaki, Y Gamano, Y Hoshi, I Shitanda, Determination of electrochemical impedance of lithium ion battery from time series data by wavelet transformation-uncertainty of resolutions in time and frequency domains. *Electrochimica Acta* **332**, 135462 (2020).
4. I Daubechies, The wavelet transform, time-frequency localization and signal analysis. *IEEE transactions on information theory* **36**, 961–1005 (1990).
5. J Allen, Short term spectral analysis, synthesis, and modification by discrete fourier transform. *IEEE Transactions on Acoust. Speech, Signal Process.* **25**, 235–238 (1977).
6. NE Huang, et al., The empirical mode decomposition and the hilbert spectrum for nonlinear and non-stationary time series analysis. *Proc. Royal Soc. London. Ser. A: mathematical, physical engineering sciences* **454**, 903–995 (1998).
7. P Flandrin, Time frequency and chirps in *Wavelet Applications VIII*. (International Society for Optics and Photonics), Vol. 4391, pp. 161–175 (2001).
8. E Chassande-Mottin, P Flandrin, On the time-frequency detection of chirps. *Appl. Comput. Harmon. Analysis* **6**, 252–281 (1999).
9. P Borgnat, P Flandrin, On the chirp decomposition of weierstrass-mandelbrot functions, and their time-frequency interpretation. *Appl. Comput. Harmon. Analysis* **15**, 134–146 (2003).
10. N Hentati, H Reckmann, I Wassermann, Identification of the channel frequency response using chirps and stepped frequencies (2008) US Patent 7,453,372.
11. K Darowicki, P Slepiski, Determination of electrode impedance by means of exponential chirp signal. *Electrochem. communications* **6**, 898–902 (2004).
12. J Verhulst, et al., System and method for impedance measurement using chirp signal injection (2017) US Patent 9,618,555.
13. P Slepiski, K Darowicki, Optimization of impedance measurements using 'chirp' type perturbation signal. *Measurement* **42**, 1220–1225 (2009).
14. FA Aroge, PS Barendse, Time-frequency analysis of the chirp response for rapid electrochemical impedance estimation in 2018 *IEEE Energy Conversion Congress and Exposition (ECCE)*. (IEEE), pp. 2047–2052 (2018).
15. B Boashash, Estimating and interpreting the instantaneous frequency of a signal. I. Fundamentals. *Proc. IEEE* **80**, 520–538 (1992).
16. PJ Loughlin, B Tacer, Comments on the interpretation of instantaneous frequency. *IEEE Signal Process. Lett.* **4**, 123–125 (1997).
17. U Khankhoje, V Gadre, Optimal fractional fourier domains for quadratic chirps. *IETE journal research* **52**, 65–70 (2006).
18. B Bullocks, R Suresh, R Rengaswamy, Rapid impedance measurement using chirp signals for electrochemical system analysis. *Comput. & Chem. Eng.* **106**, 421–436 (2017).
19. R Suresh, S Swaminathan, R Rengaswamy, Rapid impedance spectroscopy using dual phase shifted chirp signals for electrochemical applications. *Int. J. Hydrog. Energy* **45**, 10536–10548 (2020).
20. BY Chang, SM Park, Electrochemical impedance spectroscopy. *Annu. Rev. Anal. Chem.* **3**, 207–229 (2010).
21. AE Kennelly, Impedance. *Transactions Am. Inst. Electr. Eng.* **X**, 175–216 (1893).
22. D Ribeiro, J Abrantes, Application of electrochemical impedance spectroscopy (EIS) to monitor the corrosion of reinforced concrete: a new approach. *Constr. Build. Mater.* **111**, 98–104 (2016).
23. P Roberge, V Sastri, On-line corrosion monitoring with electrochemical impedance spectroscopy. *Corrosion* **50**, 744–754 (1994).
24. AM Johnson, DR Sadoway, MJ Cima, R Langer, Design and testing of an impedance-based sensor for monitoring drug delivery. *J. Electrochem. Soc.* **152**, H6 (2004).
25. C Clausen, SA Lewis, JM Diamond, Impedance analysis of a tight epithelium using a distributed resistance model. *Biophys. journal* **26**, 291–317 (1979).
26. S Ghasemi, MT Darestani, Z Abdollahi, VG Gomes, Online monitoring of emulsion polymerization using electrical impedance spectroscopy. *Polym. Int.* **64**, 66–75 (2015).
27. VGM Annamdas, Y Yang, CK Soh, Impedance based concrete monitoring using embedded pzt sensors. *Int. J. Civ. & Struct. Eng.* **1**, 414–424 (2010).
28. S Rubene, M Vilnitis, J Noviks, Frequency analysis for EIS measurements in autoclaved aerated concrete constructions. *Procedia Eng.* **108**, 647–654 (2015).
29. P Deurenberg, et al., The validity of predicted body fat percentage from body mass index and from impedance in samples of five european populations. *Eur. journal clinical nutrition* **55**, 973–979 (2001).